

TEST SECTION PRESSURE MEASUREMENTS AT THE RESEARCH WIND TUNNEL OF THE AERONAUTICAL INSTITUTE OF TECHNOLOGY

Marcelo Assato
Nide G. C. R. Fico Jr*
Roberto M. Girardi
Instituto Tecnológico de Aeronáutica – ITA
Departamento de Aeronáutica – IEAA
12228-900 - São José dos Campos - SP – Brazil
* Corresponding author, e-mail: nide@aer.ita.br

Abstract. *This work presents pressure measurements at test section of ITA´s subsonic open-circuit research wind tunnel. The test section, rectangular in shape, is 1.2 m wide, 1.0 m high and 4.0 m long. The contraction ratio is 10:1. The maximum velocity at the test section is approximately 70 m/s, which corresponds to a Reynolds number (Re) around 10^6 considering an airfoil with chord of 0.3 m. Test section dynamic pressure variations with the fan rotational speed were measured using two techniques: Pitot-Prandtl tube and two rings of static orifices (a ring at the settling chamber and the other one at the test section). Results were obtained over a complete operational rate of the tunnel. Dynamic pressure uniformities at the test section transversal area also are shown.*

Keywords*. subsonic flow, open circuit wind tunnel, flow quality, dynamic pressure, uniformity*

1. Introduction

At the Instituto Tecnológico de Aeronáutica (ITA) a low-speed non-returning wind tunnel was designed and built in a joint effort involving the Instituto Tecnológico de Aeronáutica, ITA and the Empresa Brasileira de Aeronáutica, EMBRAER. The financial support for such enterprise is given by FAPESP, Fundação de Amparo a Pesquisa do Estado de São Paulo, and by EMBRAER itself. The wind tunnel has been built as a research tool to support new developments for the aeronautical industry. A complete description of the tunnel is provided in Girardi et al. (2002). The first step after the construction of a wind tunnel is to determine its flow characteristics, and thus, verify if the flow meets the project's requirements. This process involves a thorough flow quality investigation. ITA's wind tunnel is equipped with a four-meter long test section with a rectangular cross-section which is 1.2 m wide x 1.0 m high. The flow is fed to the test section by a 10:1 contraction, designed using numerical tools (Mattos et al., 2003). As it is well-know, one of the disadvantages of open-circuit wind tunnel is the strong disturbances that the outside flow may exert upon the test-section flow. This was one of the primary concerns during the project. Therefore, in order to study such influences a 1:10 model of the tunnel's inlet section was constructed. As a result of that experimental investigation a streamlined air intake section was conceived (Assato et al., 2003).

The evaluation of the flow characteristics is undertaken with an empty tunnel test section, and has as objective to calibrate, verify and document all flow characteristics within the test section. The calibration provides correction factors or adjustments to be applied to measured aerodynamic data. This important phase of a wind tunnel is documented in the literature. The interested reader should be aware of important works by Wittwer and Moller, (2000), by Blessmann (1992) and also by Henderson and McKinney (1993).

The objective of the present paper is to present a systematic approach for the calibration open-circuit wind tunnels. The results to be shown here are related to pressure measurements correlation at different tunnel locations. These results are extremely useful during the tunnel normal operation as it will be used, for example, to determine the flow speed at the model's location.

2. Brief Description of ITA's wind tunnel and of experimental techniques

The wind tunnel built at ITA is a low-speed open-circuit tunnel. As all non-returning facilities, it has as an advantage, its low building price, and continuous fresh air at the test section, a characteristic that comes in handy when using smoke for flow visualization experiments. However, the test section flow quality is potentially affected by external winds. This sensitivity becomes especially critical at low-test speeds. Therefore, the designers carefully focused their attention to both ends of the tunnel. Figure 1 shows the 40-meter long facility. The air enters the tunnel through its inlet section, continuing into the contraction, settling chamber, and the test section. All of these tunnel's elements are housed inside the laboratory's building. Further, the test section is inside a pressure sealed 25 m x 10 m room. After reaching the test section the flow enters the diffuser, the fan section, and the exit section all mounted outside the laboratory. Notice the inlet section particular geometry. As already mentioned, it was a result of a very thorough experimental work (Assato et al., 2003). The turbulence level at wind tunnel inlet section was significantly diminished by the proposed inlet shape. In order to reduce the external wind effect at the test section (Girardi et al., 2002) a chamber was built at the other end of the tunnel. This chamber deviates the exiting air upward with the help of several guiding vanes used to minimize pressure losses. The 4.0 meter long test section is equipped with three windows at the top and three lateral ones for flow visualization with the help of a particle image velocimetry system. To ensure good flow quality along the test section, the tunnel is equipped with a stilling chamber inside which a honeycomb and three anti-turbulence screens are mounted. There is provision for an extra screen. Another important factor to guarantee a low turbulence level at the test section is a good contraction ratio. ITA's Research Tunnel is equipped with a 10: 1 contraction. In short, the tunnel's design was carefully conceived to minimize all undesirable features of non-returning wind tunnels.

To measure the total, static and dynamic pressures, two methods were utilized: (i) a Standard Pitot-static tube has been positioned within the test section with the help of a traversing, and (ii) a system with two rings of static holes. The pressure Ring 1 is located inside the stilling chamber a location where the flow velocity is very low and the measured pressure at the wall is approximately the total pressure. The other pressure Ring, shown also in Fig. 1, is placed at the test section entrance test section and actually measures the flow static pressure. Out of the data correlation made with these data it is possible to calibrate the tunnel, knowing the velocity at the test section during a particular run.

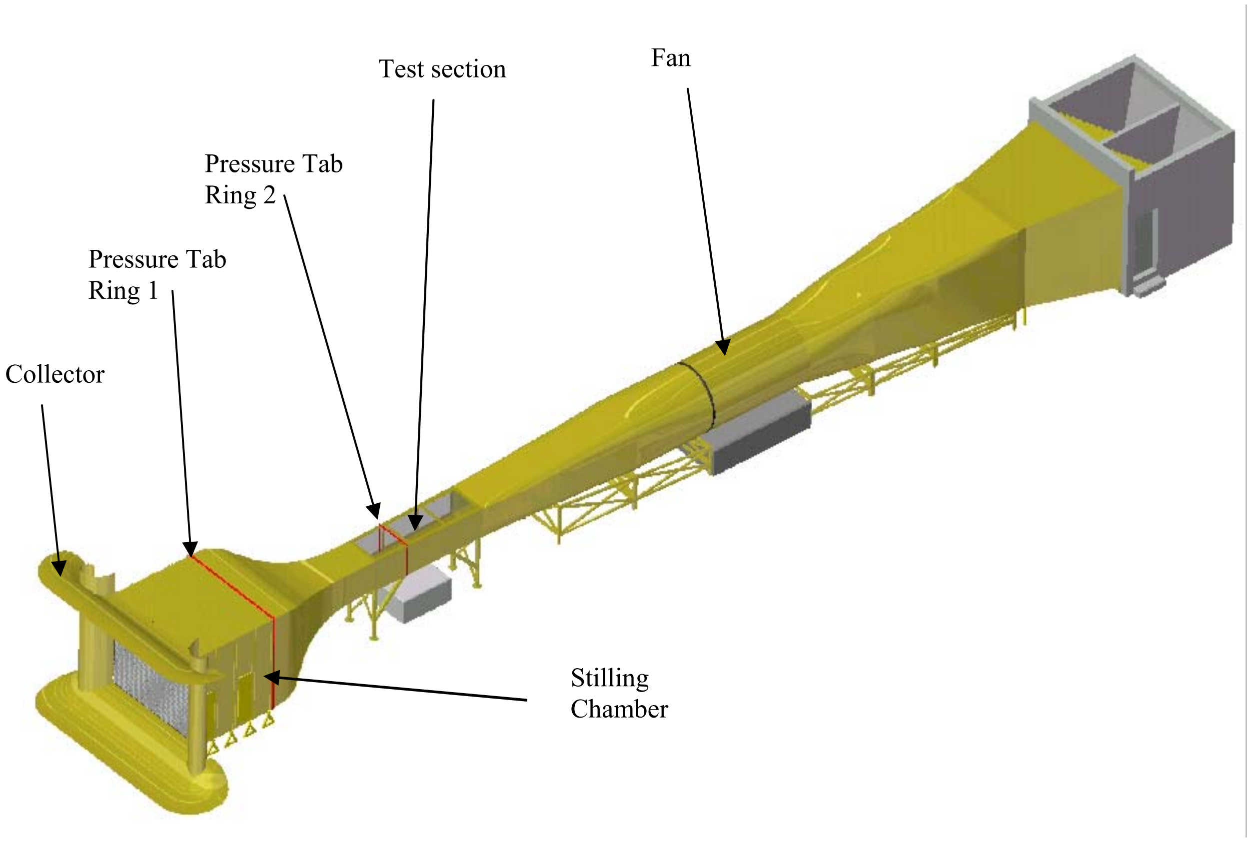

Figure 1. ITA wind tunnel.

Figure 2 shows the Pitot tube mounted at the test section. It is placed at the center of the rectangular cross-section and at midway along the test section. The Pitot was carefully aligned to the tunnel centerline with the help of a theodolite. A data acquisition system, working at a rate of 60,000 readings per minute for each measurement, was used. Pressure transducer calibration, for the range of interest, was done every day before taking measurements. The results were obtained for the whole fan rotational speed range, with 50rpm increments up to the maximum value of 890 rpm. All the tests were made by increasing the fan speed up to 890 rpm, and decreasing it back to zero rpm. Hysterisis problems were not observed.

Figure 2. Pitot-static tube.

3. Results

3.1. Analysis of the static pressure measured with Pitot tube and ring of static holes

Figure 3 shows the difference between the static pressure measured by Pitot tube and the ring of static holes (Ring 2) designated by $(P_{st})_p$ and $(P_{st})_r$, respectively. Pitot tube is always fixed at the center of the test section. The static pressure at the second ring location is systematically lower than at the center of the test section, corresponding to a greater velocity. The location of that particular pressure ring, at the test section entrance may explain the measured difference. It is located at the beginning of the test section, a region of velocity overshoot (Morel, 1975). It can be observed from Fig. 3 that as it is increased the fan speed, the difference between the static pressures given by two techniques also increases. Figure 4 is a show a plot both $(P_{st})_p$ and $(P_{st})_r$ against the atmospheric pressure. In order to double check, the pressure difference, directly measured in Fig., 3(a) was calculated based upon the data of Fig. 4 and presented in Fig. 4(b). It can be observed the same trend as Fig. 3.

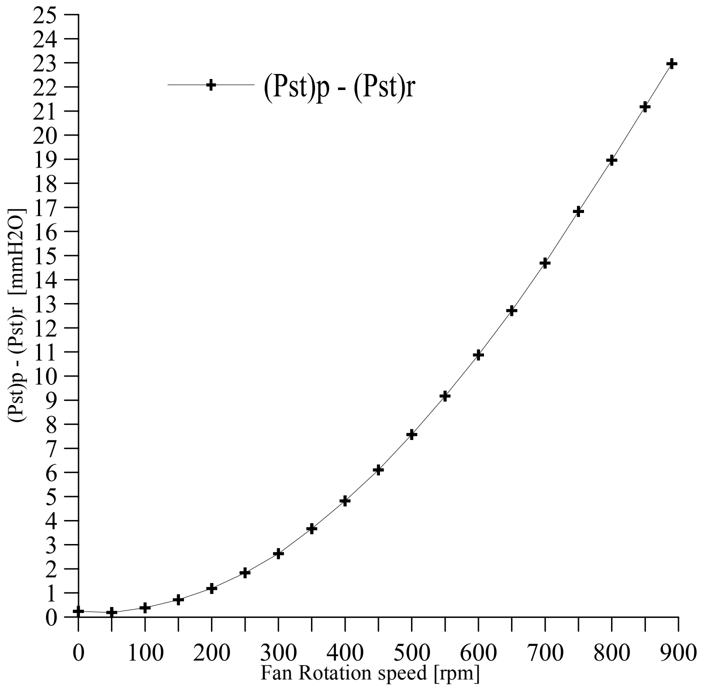

Figure 3. Difference the static pressure measured by Pitot tube and ring 2.

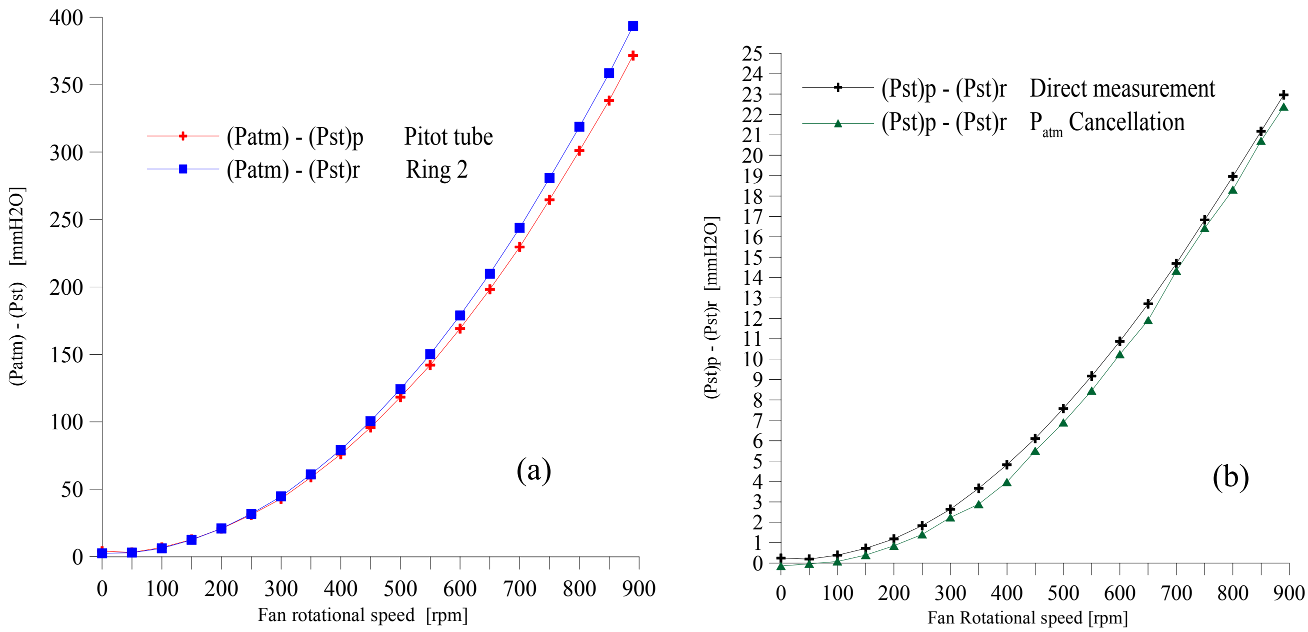

Figure 4. (a) Difference between the atmospheric pressure and the static pressure measured by Pitot tube and ring 2. (b) comparison between the difference of Pitot and ring static pressure given by the direct way and cancellation of the atmospheric pressure.

3.2. Analysis of the total pressure measured with Pitot tube and ring of static holes

The total pressure measured by the first ring was also calibrated against the Pitot data. The total pressure measured by the Pitot, $(P_t)_p$, minus the total pressure measured at the first ring, $(P_t)_r$, is plotted against the fan rotational speed, see Fig. 5. As mentioned before the pressure reading at the first ring is an approximation of the total pressure due to the low flow speed at the tunnel's settling chamber. Thus, it is expected that the Pitot readings will be higher than those of the ring. Indeed, that is confirmed by looking at Fig. 5 as well as Fig. 6.

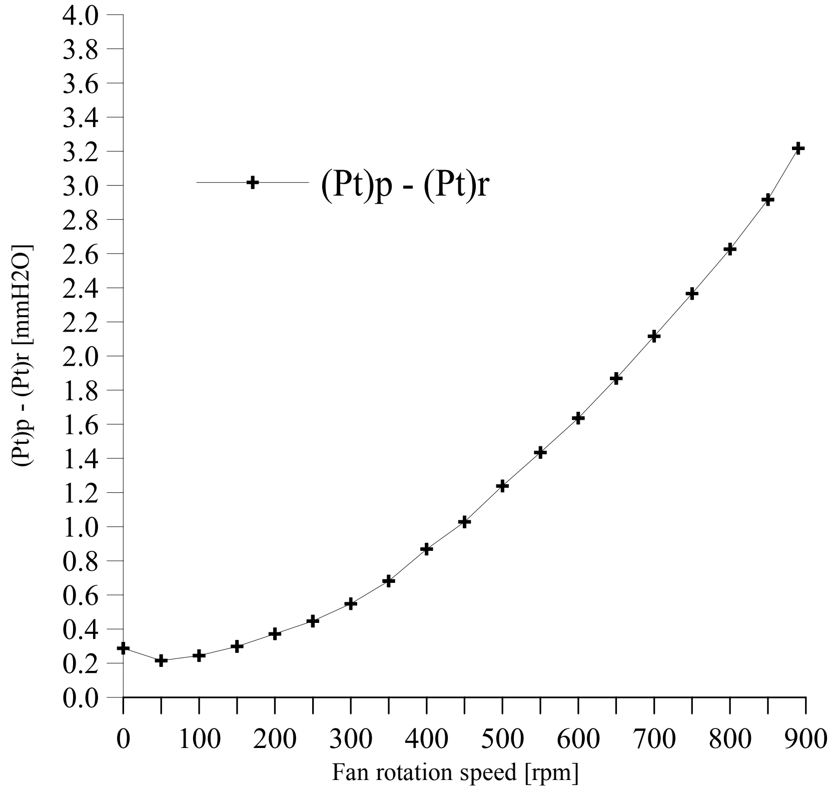

Figure 5. Difference the total pressure measured by Pitot tube and ring 1.

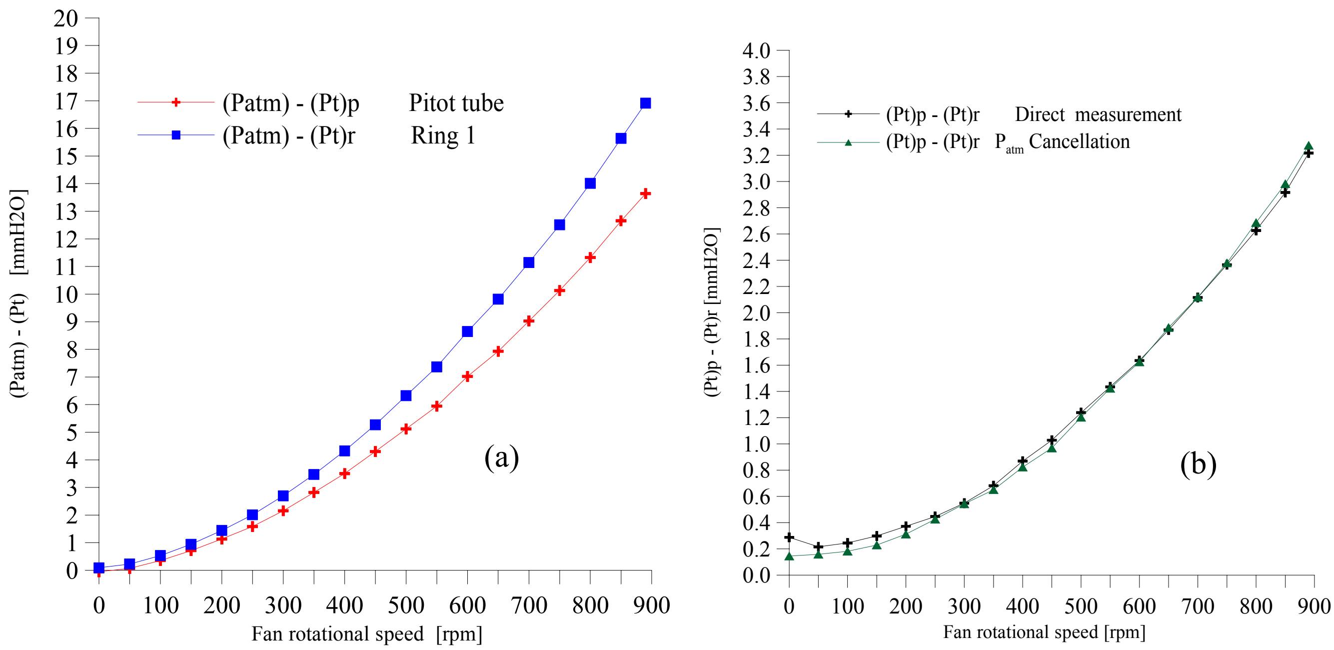

Figure 6. (a) Difference between the atmospheric pressure and the total pressure measured by Pitot tube and ring 1. (b) comparison between the difference of Pitot and ring total pressure given by the direct way and cancellation of the atmospheric pressure.

3.3. Analysis of the dynamic pressure measured with Pitot tube and ring of static holes

A very important pressure data is shown in Fig. 7. In this particular figure a plot of the dynamic pressure measured with the Pitot tube and using both rings are plotted against the fan rotational speed that varies from zero to its maximum value of 890 rpm. As all other curves shown, the measurements were made increasing the fan speed up to 890 rpm, and decreasing it back to zero rpm. Hysterisis problems were not observed.

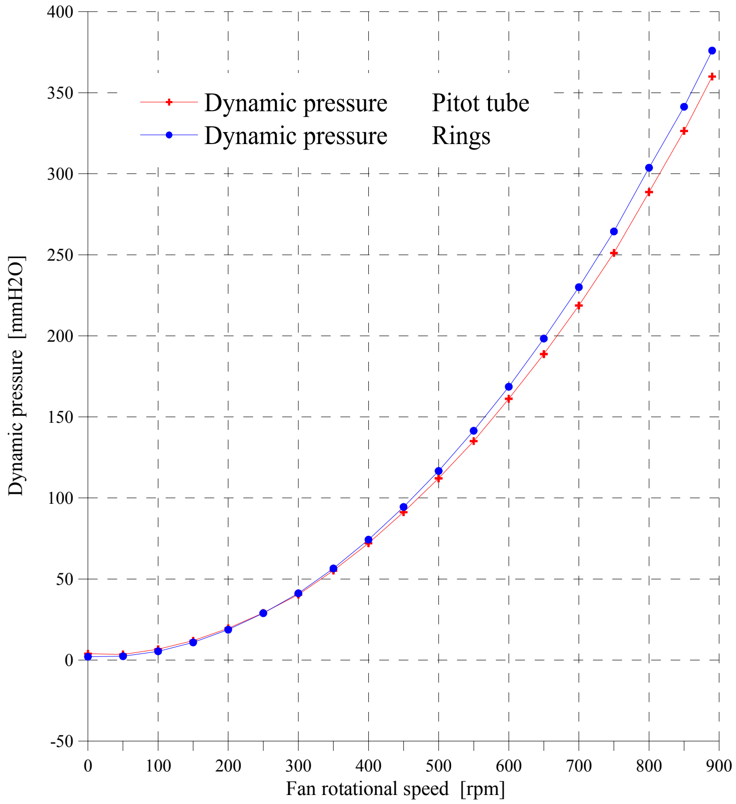

Figure 7. Dynamic pressure measured by Pitot tube and rings.

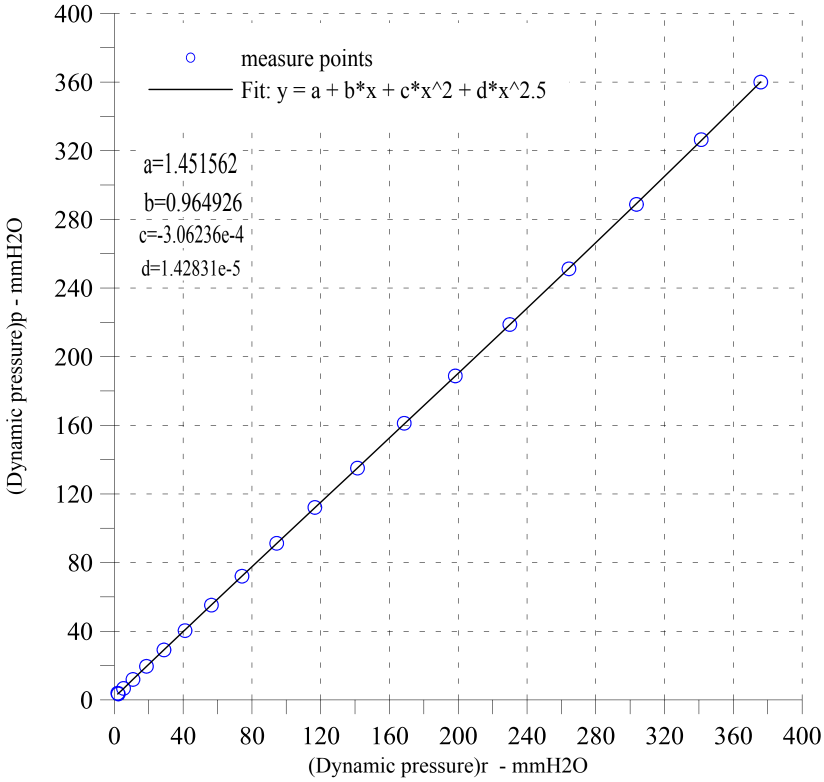

Figure 8. Correlation between the dynamic pressure measured by Pitot and rings.

3.4. Preliminary Flow Uniformity Results

Next, a detailed description of the experimental procedure to determine flow uniformity at a cross-section of the test section is given. For the preliminary results shown hereafter attention will be focus at a cross-section located halfway along the test-section that is 2 meters away form its entrance plane. Following Barlow, Rae and Pope (1999) the local dynamic pressure must not deviate more than 0.50% from the mean dynamic pressure at the particular cross-section of interest. Applying the same criteria to the velocity vector magnitude leads to a 0.25% deviation from the mean cross-section velocity. These strict requirements call upon extra care in obtaining the experimental data. In other words, the experimental procedure must be well suited for this particular application. One must be aware that any interference, even small ones, may disturb the flow and produce misleading results. For example, the Pitot tube positioning system, shown in Fig. 2, is an interference source. During this early stage of the calibration phase it has been observed the sensitiveness of the pressure readings in respect to the positioning system location. Figure 9 shows the voltage output for the dynamic pressure, measured with both the Pitot tube and the pressure rings, as the Pitot is traversed throughout the lower right-hand quarter of the tunnel cross section, keeping the fan rotational speed fixed at 400 rpm. The sweep, done at 5 cm intervals, starts at the top of the test section. A total of 9 points are read at each span wise station. It is clear; from Fig. 9 that both pressure transducers output varies according to the position of the Pitot tube. The minimum voltage output is associated with the point located along the test-section horizontal symmetry line. This behavior was observed for both the dynamic pressure measured using the rings as well as the Pitot tube. One would expect that the pressure rings reading would present only a slight variation, within the experimental uncertainty. Further, it would also be expected that such variation would be independent of the Pitot tube location. This is particularly true if one recalls that all measurements were taken at a fixed fan rotational speed. The authors believe that the positioning system is somehow introducing a different pressure loss depending upon the location it occupies inside the test section. This, in turn, would alter the flow rate.

An open-circuit wind tunnel is affected by external wind gusts, especially at low test-section speeds (Eckert et al. 1976, Whitehouse, 1983). That is one of the reasons these first results flow uniformity were obtained at a fan rotational speed of 400 rpm. Since the beginning of the tunnel's calibration a slight air drift has been noticed at the test section when the fan is off. To minimize this influence upon the pressure readings, notably for low-speed flow, pressure readings are made with the fan off. The calibration curves for the pressure transducers are obtained offsetting all voltage values with respect to the fan-off reading.

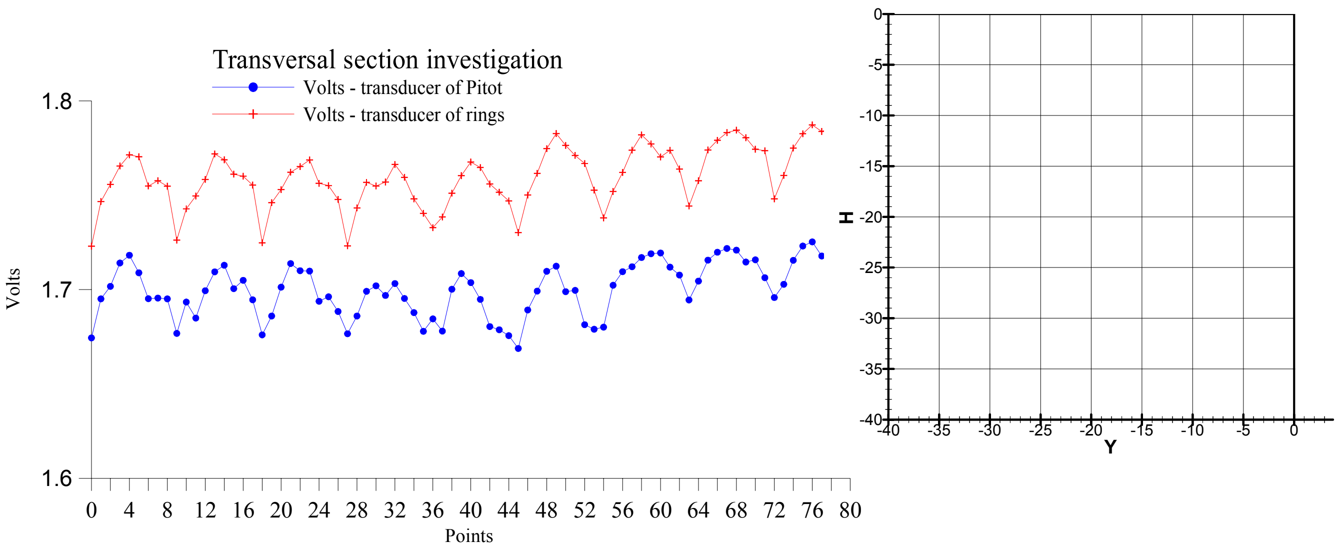

(a) (b)

Figure 9. (a) Voltage variation obtained by the Pitot transducers and by the pressure tab rings during a cross-sectional sweep. The points along the ordinate correspond to the grid shown. (b) Cross-section investigated.

That is,

$$P_i = a(V_i - V_0),\tag{1}$$

where P_i is the pressure, V_i the voltage related to P_i and V_o the fan-off voltage output.

Another very important aspect of the transducers calibration is the chosen pressure range used in such procedure. The choice of a small pressure the calibration range minimizes the experimental uncertainty on the velocity measurements. For the results presented hereafter the fan rotational speed was set at 400rpm, corresponding to a 70 mmH_20 dynamic pressure. In this particular case the calibration range was chosen from 60 to 80 mmH_20. The uncertainty on the velocity data is, in turn, $\Delta V = \pm 0.04 m/s$.

In order to minimize the above-mentioned interferences it was decided to use a non dimensional velocity given by $\Lambda = V_p / V_r$, being the numerator the velocity calculated from the Pitot reading and the denominator the velocity obtained with the ring pressure data. This parameter is used to calculated the deviation form the mean and thus find the velocity uniformity at the cross-section. Such a procedure was adopted after the authors observed variation of more than 10 mmH_20 during a trial velocity uniformity mapping.

Figure 10 shows preliminary results of the flow uniformity at the inferior left quadrant of the cross section located exactly midway along the test section length. The velocity vector magnitude varies within $\pm 0.5\%$ of tits mean value at the particular cross section investigated. In Fig. 10 (a) it may be observed that exists two "odd points" that deviate considerably from the mean cross-sectional average value. Discarding these two points and interpolating them in function of their neighbors it is observed, in the 10 figure (b), that all the distribution is affected. Discarding these two points, that may have been affected by an expourious influence, gives the overall distribution a smoother looking. Further, the author's noticed that the greatest variations coincide with the positions where the experimental was stopped only to be re-started the next day. This "over night" non-uniformity is currently being investigated.

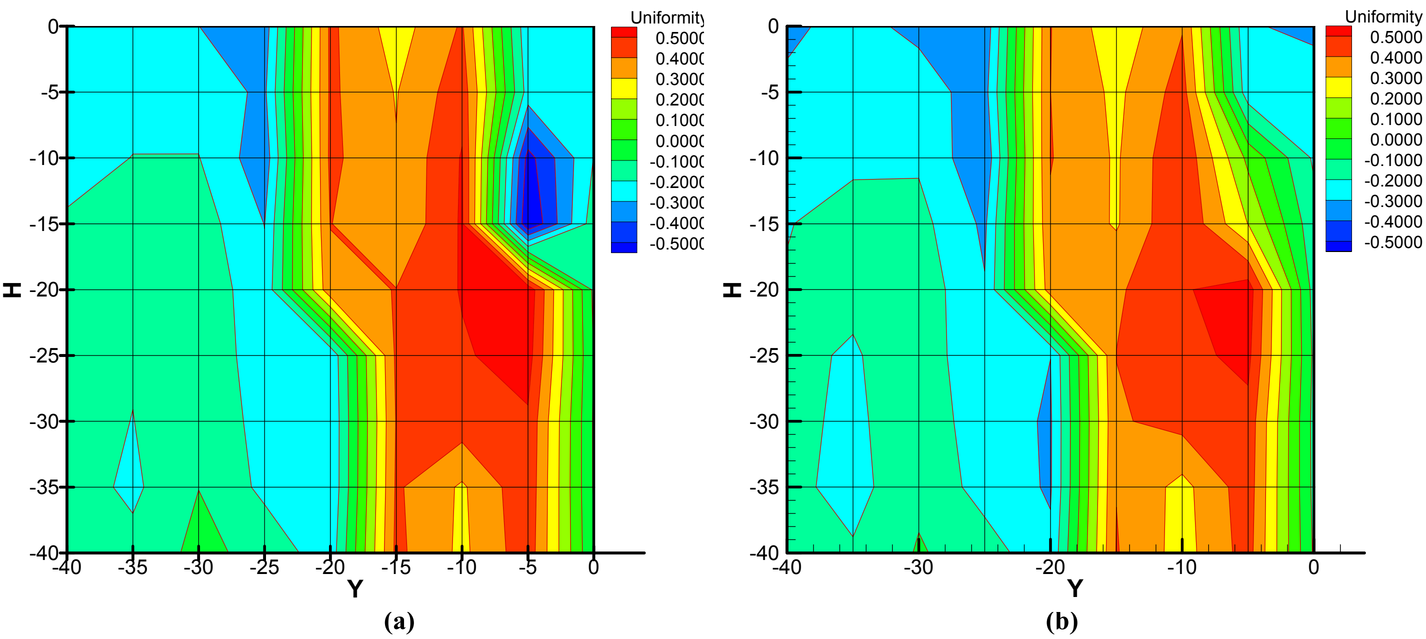

Figure 10. Velocity distribution at the inferior left cross-section quadrant.

3.5. Longitudinal pressure gradient along the test section

According to Barlow, Rae and Pope (1999) the static pressure gradient along the test section must be known in order to make necessary buoyancy corrections. To measure it a long pipe with several static pressure holes is used. The tube used is 1.60 m long and the pressure reading is made at every 5 centimeters. Figure 11 shows the measuring device installed and lined up inside the test section. It is very important to have it perfectly aligned with the flow to make sure that the pressure being measured is indeed the static pressure. Numerous pressure readings were carried out for several test-section dynamic pressures. Another precaution taken was to turn the static pressure pipe in respect to its symmetry axis to make sure that there was no misalignment of the pipe and also make sure that the pipe supporting structure, seen in Fig. 11, was not an interference source.

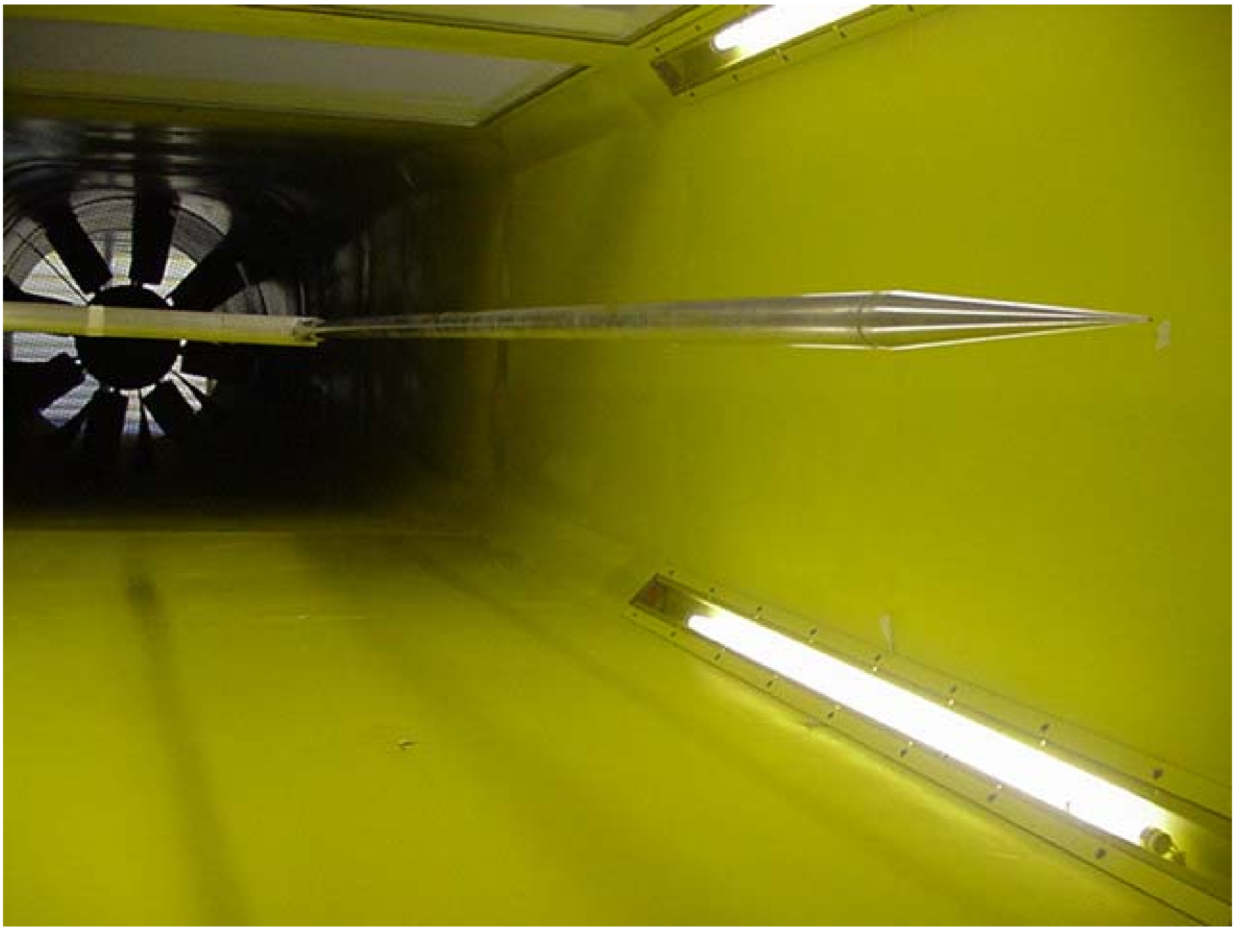

Figure 11. Long static tube inside the test section.

The static-pressure data acquisition was made using a HBM module and two electronic sensors of different operating ranges: one was a PSI of 10"WC model 3271A, and another a PSI of 1 psi model 32721A. Figure 12 shows the sensor mounted and ready to go. It is important to emphasize that all pressure measurements were taken simultaneously. This experimental procedure is very important in open-circuit wind tunnels as it eliminates external wind interference that would most certainly occur if the pressure readings were made sequentially.

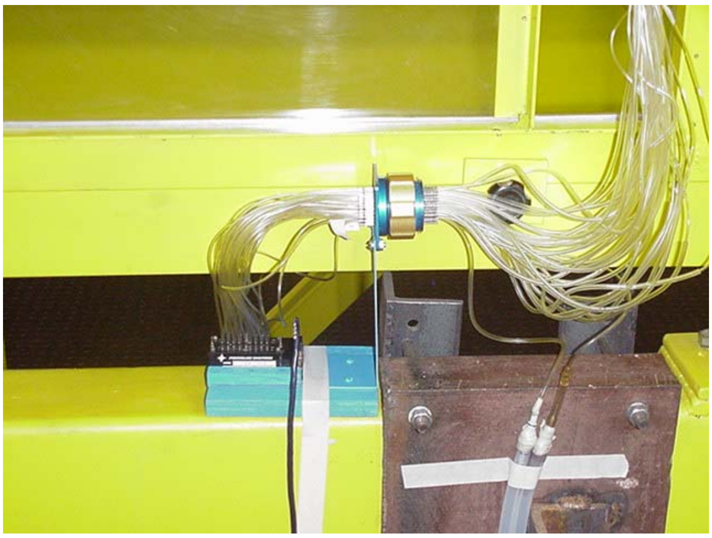

Figure 12. PSI electronic sensor mounted outside the tunnel.

Figures 13 and 14 show the static-pressure distributions, along the test section, measured by the long static pipe. Actually, the plotted variable is the measured pressure minus the atmospheric pressure divided by the test-section dynamic pressure. It is observed in Fig. 13 that for low dynamic pressure, corresponding to a fan speed lower than 200 rpm, the external-wind influence is an important factor. For higher fan rotational speeds such effect becomes very small the non-dimensionalized results practically coincide, see Fig 14.

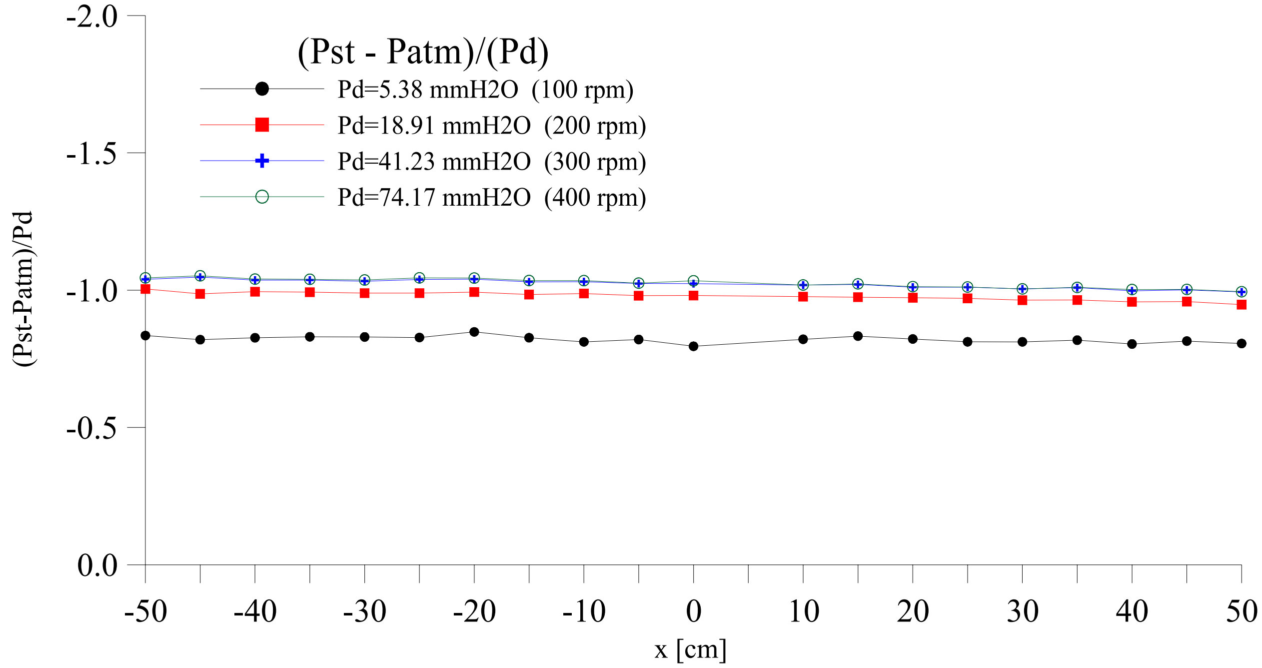

Figure 13. Static pressure distribution along the test section for rotations of the fan from 100 to 400 rpm

It was also observed that static-pressure gradient is positive in the flow direction. During the design phase, the test section divergence angle was calculated to compensate for the boundary layer growth along the four-meter test section. However, the present experiment results show that there was an over-compensation for the boundary-layer growth Foreseeing this type of problem, the test section was provided with removable corner fillets that can replaced until the become static-pressure gradient becomes acceptably small.

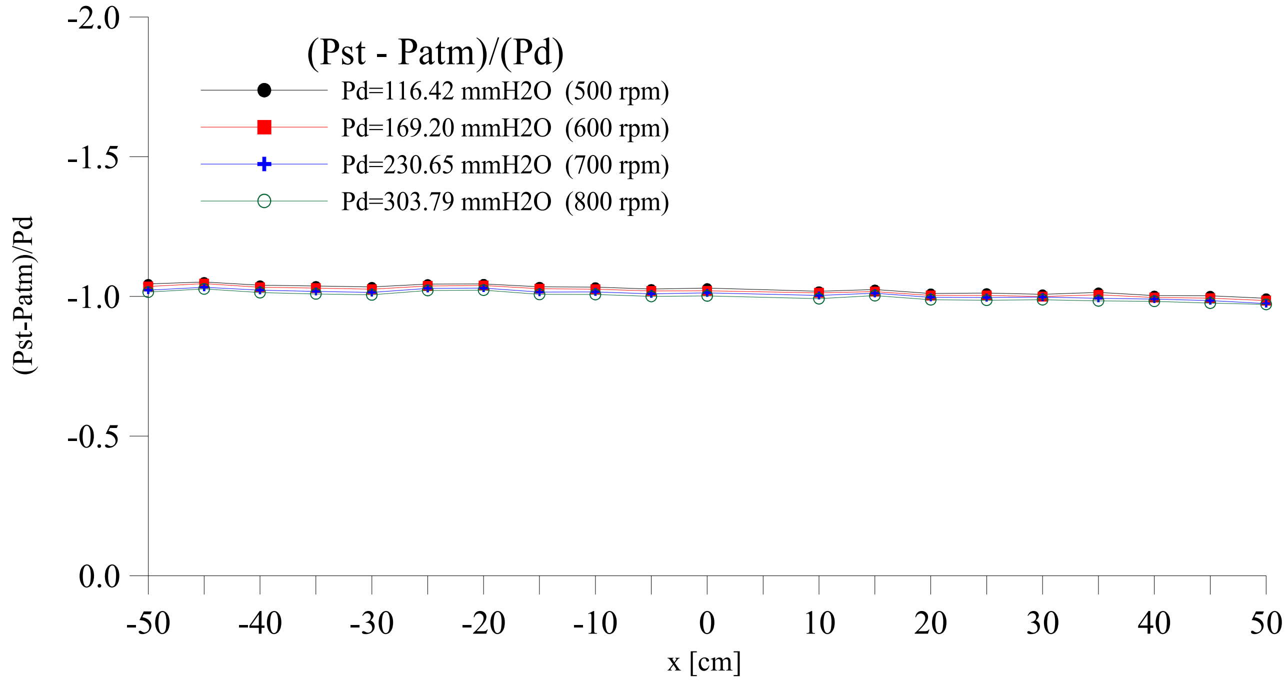

Figure 14. Static pressure distribution along the test section for rotations of the fan from 500 to 800 rpm

4. Conclusion

This work reports experimental procedures during the calibration phase of an open-circuit wind tunnel as well as preliminary pressure measurements in the test section of the Research Wind Tunnel of the Technological Institute of Aeronautics, ITA. Total, static and dynamic pressures have been measured for several fan rotations, covering the whole operating tunnel envelope. Two different techniques to measure pressures were used and the results compared. An equation for dynamic pressure correlation was obtained based upon the results of these two measuring methods. The difficulties to map the flow uniformity at a tunnel cross-section have been shown and commented in this work. Preliminary results have indicated good flow uniformity. The static-pressure gradient along the test section has been measured. Results indicated the existence of a gradual static-pressure decrease along the test section length. The tunnel calibration phase is just starting. As it progresses more will be learned about the test section flow as well as about the unique experimental procedures related to open-circuit wind tunnels.

5. Acknowledgement

To the Fundação de Amparo a Pesquisa do Estado de São Paulo (FAPESP), for supporting part of the resources used to built this wind tunnel (project: FAPESP 00/13769-0). To EMBRAER for supporting the modifications required to the infra-structure of the Prof. K.W. Feng Aeronautical Engineering Laboratory and to Carlos Guedes Neto, Luis Zambrano Lara, Vitor Valentim Betti and Mario Correia, members of the above mentioned laboratory.

6. References

Assato, M., Fico Jr, N.G.C.R and Girardi, R.M., 2003, "Experimental Study of the Turbulence Level at the Intake of an Open Circuit Wind Tunnel", Paper AIAA-2003-3948, 21st AIAA - Applied Aerodynamics Conference, 23 - 26 Jun, Session 86: Wind Tunnel Aerodynamics and Experimental Studies II, Orlando, Florida, USA.

Eckert, W. T., Mort, K. W. and Piazza, J. E., 1976, "An Experimental Investigations of End Treatments for Nonreturn Wind Tunnels", NASA Technical Memorandum, NASA TM X-3402.

Barlow, J.B., Rae. W. H. Jr. and Pope, A., 1999, Low Speed Wind Tunnel Testing, John&Sons, Third Edition, Inc.

Blessmann, J., 1982, "The boundary layer TV2 Wind Tunnel of the UFRGS", Journal of Wind Engineering and Industrial Aerodynamics (10), pp. 231-248.

Girardi, R. M., Fico, Jr, N.G.C.R., Mello, O. A. F. and Komatsu, P., 2002, "Projeto do Túnel de Vento Subsônico de Pesquisa do Instituto Tecnológico de Aeronáutica", In: CONEM2002 - II Congresso Nacional de Engenharia Mecânica, 19-23 Ago 2002, V. CDROM, João Pessoa, Brasil.

Henderson Jr., A. and McKinney L.W., 1993, "Overview of the 1989 Wind Tunnel Calibration Workshop", NASA Technical, Paper NASA-TP-3393, pp.45.

Mattos, B., Fico Jr, N.G.C.R and Girardi, R.M., 2003, "Design of the Contraction of ITA's Research Wind Tunnel Using CFD Tolls", Paper AIAA-2003-3949, 21st AIAA - Applied Aerodynamics Conference, 23 - 26 Jun, Session 86: Wind Tunnel Aerodynamics and Experimental Studies II, Orlando, Florida, USA.

Morel, T., 1975, "Comprehensive Design of Axisymmetric Wind Tunnel Contractions," Journal of Fluids Engineering, pp225-233.

Wittwer, A. R. and Moller, S. V., 2000, "Characteristics of the Low-Speed Wind Tunnel of the UNNE", Journal of Wind Engineering and Industrial Aerodynamics (84), pp. 307-320.

Whitehouse, I. R., 1983, "Tests to Determine the Influence of Natural Wind Direction on the Working Section Flow Characteristics of an Open Return Type Wind Tunnel", M. Sc. Thesis, College of Aeronautics, Cranfield Institute of Technology, England.